PNAS RESEARCH ARTICLE | GENETICS

Retinoic acid receptor α activity in proximal tubules prevents kidney injury and fibrosis

Krysta M. DiKun[a,b], Xiao-Han Tang[a], Leiping Fu[a], Mary E. Choi[c,d], Changyuan Lu[e], and Lorraine J. Gudas[a,b,f,1]

Edited by David Moore, University of California Berkeley, Berkeley, CA; received July 11, 2023; accepted December 18, 2023

Chronic kidney disease (CKD) is characterized by a gradual loss of kidney function and affects ~13.4% of the global population. Progressive tubulointerstitial fibrosis, driven in part by proximal tubule (PT) damage, is a hallmark of late stages of CKD and contributes to the development of kidney failure, for which there are limited treatment options. Normal kidney development requires signaling by vitamin A (retinol), which is metabolized to retinoic acid (RA), an endogenous agonist for the RA receptors (RARα, β, γ). RARα levels are decreased in a mouse model of diabetic nephropathy and restored with RA administration; additionally, RA treatment reduced fibrosis. We developed a mouse model in which a spatiotemporal (tamoxifen-inducible) deletion of RARα in kidney PT cells of adult mice causes mitochondrial dysfunction, massive PT injury, and apoptosis without the use of additional nephrotoxic substances. Long-term effects (3 to 4.5 mo) of RARα deletion include increased PT secretion of transforming growth factor β1, inflammation, interstitial fibrosis, and decreased kidney function, all of which are major features of human CKD. Therefore, RARα's actions in PTs are crucial for PT homeostasis, and loss of RARα causes injury and a key CKD phenotype.

kidney disease | retinoic acid | proximal tubule | fibrosis | mitochondria

Significance

Progressive renal fibrosis is a hallmark of late stages of chronic kidney disease (CKD), contributing to the development of kidney failure. Slowing or reversing fibrosis could potentially return CKD kidneys to a healthy state. However, there are few US Food and Drug Administration (FDA)-approved drugs that treat renal fibrosis. Our data indicate that (retinoic acid receptor) RARα's actions in proximal tubules (PTs) are crucial for PT homeostasis and that selective loss of RARα in PTs leads to inflammation and fibrosis. Therapies that selectively activate RARα in the kidney could maximize anti-fibrotic effects in renal tissue while reducing potential side effects.

Chronic kidney disease (CKD) has a global prevalence of 13.4% and is characterized by a gradual loss of kidney function persisting longer than 3 mo (1). The main pathological features of CKD include glomerulosclerosis, tubular atrophy, and a high degree of tubulointerstitial fibrosis (2). CKD is divided into five stages based on glomerular filtration rate and albuminuria, with stage 5 indicating progression to end-stage renal disease (3). People with CKD are 5 to 10 times more likely to die from a comorbidity, such as cardiovascular disease, before reaching stage 5 (2, 4). With early interventions, such as lifestyle changes and medications that regulate blood pressure and glucose levels, it may be possible to slow CKD progression (1, 3). However, over 90% of those affected are asymptomatic and unaware that they have CKD until their kidneys have become irreversibly fibrotic (5). At this stage, many patients must undergo dialysis or kidney replacement, as there are very few approved drugs that treat renal fibrosis.

The onset of CKD can follow an acute kidney injury (AKI), particularly involving the proximal tubules (PTs), caused by ischemia, obstruction, or toxic chemicals (6). In fact, the severity and frequency of PT injury influences progression to CKD (7). Following injury, surviving PT cells enter a repair cycle which leads to transient production and secretion of profibrotic growth factors, such as TGF-β1 (transforming growth factor β1), to promote wound healing via fibroblast proliferation and extracellular matrix (ECM) secretion (8, 9). In instances of sustained injury, prolonged secretion of TGF-β1 causes the trans-differentiation of residential fibroblasts into myofibroblasts (10, 11). The activation of myofibroblasts is a major driver of fibrosis through the overproduction of ECM (7). Prolonged PT injury also results in the infiltration of inflammatory cells, such as macrophages, another source of fibroblast priming and growth factor secretion (8, 12). Collectively, these and related data indicate that repeated PT injury results in interstitial fibrosis, a major hallmark of CKD (13, 14).

Vitamin A (retinol, VA), a micronutrient/vitamin obtained from food, can be metabolized to retinaldehyde, which can further be metabolized to all-trans retinoic acid (RA), an endogenous agonist for the RA receptors (RARs) α, β, γ, members of the family of nuclear receptors which act as transcription factors (15, 16). Proper RA signaling is critical for stem cell differentiation and other developmental processes (17, 18). In addition, VA plays a major role in the regeneration of PTs after external injury using agents such as diphtheria toxin (19). Retinoid levels in serum and kidney cortices are known to be altered during the onset of CKD (17, 20). The activity of RARα is required for kidney development and RARα expression is decreased in kidney cortices of mice with diabetic nephropathy (DN) and restored upon RA administration (21, 22). Nakamura et al. showed that

Author affiliations: [a]Department of Pharmacology, Weill Cornell Medical College of Cornell University, New York, NY 10065; [b]Weill Cornell Graduate School of Medical Sciences, New York, NY 10065; [c]New York Presbyterian Hospital, New York, NY 10065; [d]Division of Nephrology and Hypertension, Joan and Sanford I. Weill Department of Medicine, Weill Cornell Medicine, New York, NY 10065; [e]Quantum-Si, Guilford, CT 06437; and [f]Department of Urology, New York, NY 10065

Author contributions: K.M.D., X.-H.T., and L.J.G. designed research; K.M.D., L.F., C.L., and L.J.G. performed research; K.M.D. and X.-H.T. analyzed data; X.-H.T. and L.J.G. revised and approved the final version of manuscript for publication submission; L.F. generated the transgenic mouse model; M.E.C. provided conceptual advice; and K.M.D., X.-H.T., M.E.C., and L.J.G. wrote the paper.

The authors declare no competing interest.

This article is a PNAS Direct Submission.

[1]To whom correspondence may be addressed. Email: ljgudas@med.cornell.edu.

This article contains supporting information online at https://www.pnas.org/lookup/suppl/doi:10.1073/pnas.2311803121/-/DCSupplemental.

Published February 8, 2024.

shortly after injury-induced activation of renal myofibroblasts, these myofibroblasts transiently acquired the ability to synthesize RA via an increase in expression of the enzyme ALDH1a2 (RALDH2), which converts retinaldehyde to RA (19), demonstrating a link between RA and attenuation of fibrosis.

Here, we delineate the functions of RARα in PT cells and show that a functional RARα is necessary for PT cell survival, as RARα deletion specifically in PT cells of adult mice causes PT injury and progressive fibrosis. These findings implicate RARα as a potential therapeutic target to protect against or limit the damaging effects of renal injury and fibrosis.

Results

Generation of Tamoxifen-Inducible, PT–Specific RARα Knockout (KO) Mice. To create this model, we first developed a transgenic mouse line with a tamoxifen (tam)-inducible Cre recombinase (CreER) under a truncated (γ-glutamyl transferase 1) GGT1 promoter (abbreviated GGT-CreER) (*SI Appendix*, Fig. S1). GGT1 is specifically active in segment 1 of kidney PT cells (23, 24). To verify the specificity of this GGT1 promoter, we crossed the GGT-CreER line with ROSA transgenic mice [B6.129S4-Gt (ROSA)26Sortm1Sor/J; Jackson Labs] and confirmed that, after tam-injections, lacZ was expressed in PT cells of the kidney cortex, as shown by blue X-gal staining (*SI Appendix*, Fig. S2). We then crossed the GGT-CreER line with mice containing a floxed RARα gene (25) ($GC^{ER}RARα^{fl/fl}$) (Fig. 1*A*) and demonstrated via semi-qPCR that RARα KO ($GC^{ER}RARαΔ$) in the kidney cortex occurs after a 2-d treatment of adult mice with tamoxifen (tam); RARα knockout (KO) is detectable as early as 3 d post-tam (Fig. 1*B* and *SI Appendix*, Fig. S3). We verified that tam-injections induced RARα KO in the kidney cortex and not in other tissues such as the liver (Fig. 1*C* and *SI Appendix*, Fig. S4). Additionally, we sequenced the 316 bp excised band (*SI Appendix*, Fig. S5) and verified that it aligned with RARα cDNA (NM_001361954.1) and that the "KO region" was located within exon 4 [referred to as exon 8 by Chapellier et al. (25) using older nomenclature], which contains the DNA binding domain (*SI Appendix*, Fig. S6). To assess RARα protein, we stained kidney sections from $GC^{ER}RARα^{fl/fl}$ and $GC^{ER}RARαΔ$ mice. While we observed nuclear RARα staining in >95% of PT cells in $GC^{ER}RARα^{fl/fl}$ kidneys, we detected no RARα protein in >95% of GGT1-expressing PT cells of $GC^{ER}RARαΔ$ kidneys 3 d post-tam treatment (Fig. 1*D*). Any potential remaining protein was undetectable by immunofluorescence.

RARα Expression Is Essential for PT Homeostasis. RA influences expression of genes involved in fibrosis, proliferation, inflammation, cell differentiation, and apoptosis (26, 27). We observed that, compared to WT, $GC^{ER}RARαΔ$ PT cells exhibited a 119-fold ($P < 0.0001$) increase in apoptosis at 3 d post-tam; apoptosis subsequently decreased by 12.5-fold ($P < 0.0001$) at 3 mo post-tam compared to 3 d post-tam (Fig. 2 *A* and *B*). In response to injury,

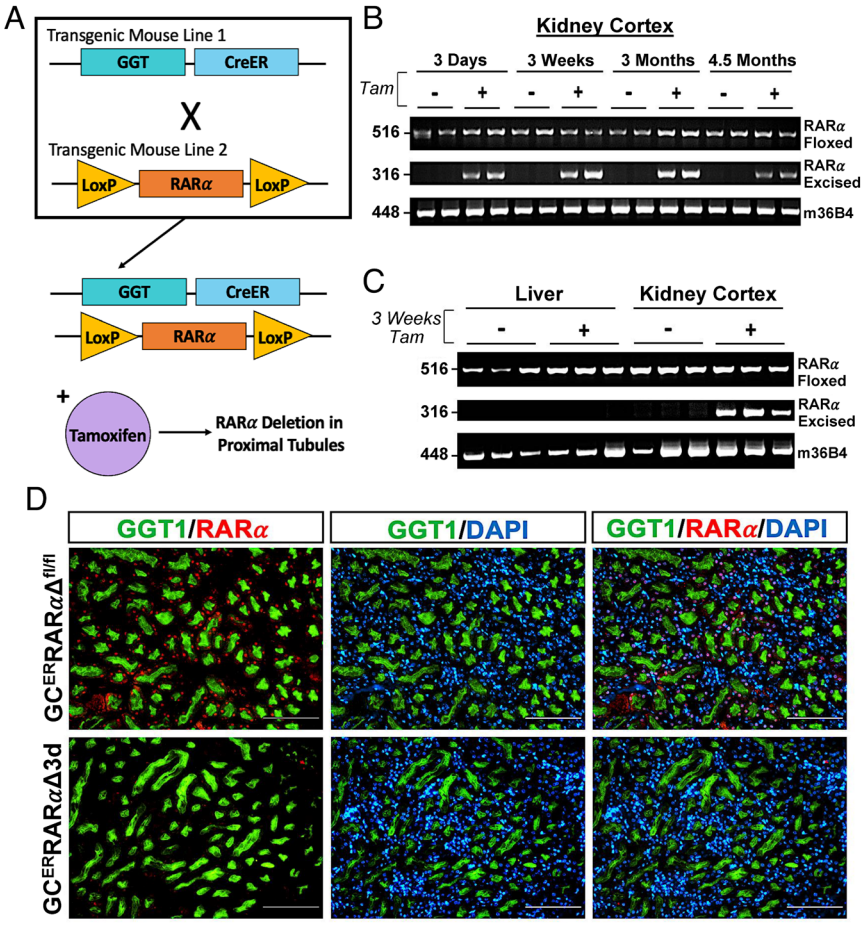

Fig. 1. Generation of tamoxifen-inducible, PT–specific RARα KO mice. (*A*) Schematic of the mouse model. (*B*) Verification of RARα excision at various time points post-tamoxifen injection; semi-quantitative PCR of genomic DNA (n = 2/group) from kidney cortices of $GC^{ER}RARα^{fl/fl}$ females with (+) or without (−) tamoxifen that were killed 3 d, 3 wk, 3 mo, or 4.5 mo post-injection. m36B4 utilized as internal control. (*C*) Verification of tissue-specific RARα excision; semi-quantitative PCR of genomic DNA (n = 3/group) from liver and kidney cortices of $GC^{ER}RARα^{fl/fl}$ females with (+) or without (−) tamoxifen that were killed 3 wk post-injection. (*D*) Representative images (8 fields/mouse) of RARα (TXRED) and GGT1 (GFP) co-stained kidney cortices from $GC^{ER}RARαΔ$ females 3 d post-tamoxifen and age-matched $GC^{ER}RARα^{fl/fl}$ females (n = 3/group). Magnification 200×. (Scale bar, 100 μm.)

PTs enter a repair pathway to restore proper nephron structure (28). This pathway involves surviving PT cells de-differentiating, during which they express CC chemokine ligand 2 (CCL2), followed by rapid proliferation, indicated by Ki67 expression, and re-differentiation (11, 29, 30). In GC^{ER}RARαΔ cortices 3 d post-tam compared to WT, proliferation increased by 3.6-fold ($P < 0.0001$) in PT cells, as identified by tubules with cuboidal epithelial cells containing abundant cytoplasm and an identifiable brush border (31); proliferation then decreased by 1.5-fold ($P < 0.0001$) in GC^{ER}RARαΔ kidneys 3 mo post-tam compared with GC^{ER}RARαΔ mice 3 d post-tam (Fig. 2 *C* and *D*). This increase in proliferation at 3 d post-tam is seen only in females (*SI Appendix*, Figs. S7 and S8).

Additionally, we observed progressive de-differentiation of PTs post-deletion of RARα, as measured by a 6.4-fold increase ($P < 0.0001$) of CCL2 in GC^{ER}RARαΔ cortices 3 d post-tam vs. WT; CCL2 increased an additional 2.1-fold ($P < 0.001$) by 3 mo post-tam (Fig. 2 *E* and *F*). There was no overlap of CCL2 staining with Lotus tetragonolobus lectin (LTL) (*SI Appendix*, Figs. S9 and S12), a marker of segments 1 to 3 of mature PTs (11) that is still expressed at comparable levels in wild-type and GC^{ER}RARαΔ mice 3 d post-tam (*SI Appendix*, Fig. S10), thus indicating two

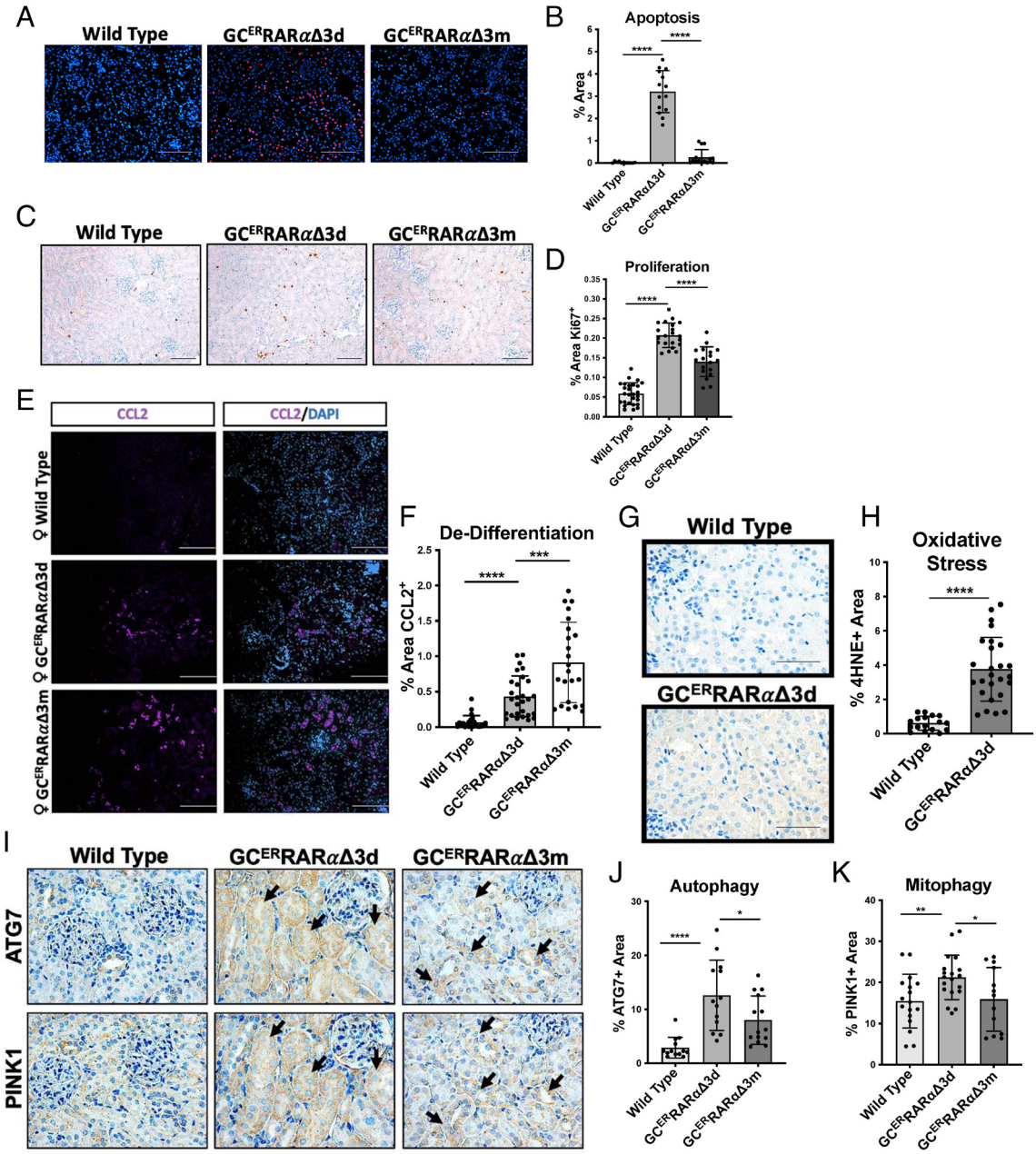

Fig. 2. RARα expression is essential for PT homeostasis, and the deletion of RARα in PTs leads to mitochondrial distress. (*A*) Representative images (4 to 5 fields/mouse) of TUNEL-stained kidney cortices from GC^{ER}RARαΔ females 3 d and 3 mo post-tamoxifen and wild-type females age matched to the GC^{ER}RARαΔ 3 mo post-tamoxifen group (n = 3/group). (*B*) Quantification of % area fluorescence from TUNEL+ cells. (*C*) Representative images (6 to 9 fields/mouse) of Ki67-stained kidney cortices from mice described in (*A*). (*D*) Quantification of Ki67+ % area. (*E*) Representative images (7 to 9 fields/mouse) of CCL2-stained kidney cortices from mice described in (*A*). (*F*) Quantification of CCL2+ % area. (*G*) Representative images (6 to 9 fields/mouse) of 4-HNE-stained kidney cortices from GC^{ER}RARαΔ females 3 d post-tamoxifen and age-matched wild-type females (n = 3/group). (*H*) Quantification of 4-HNE+ % area. (*I*) Representative images (6 to 9 fields/mouse) from similar areas of ATG7 and PINK1 stained kidney cortices from mice described in (*A*). (*J*) Quantification ATG7+ % area. (*K*) Quantification of PINK1+ % area. Magnification 200× (*A*, *C*, and *E*) with a 100-μm scale bar or 600× (*G* and *I*) with a 50-μm scale bar. *$P < 0.05$, **$P < 0.01$, ***$P < 0.001$, and ****$P < 0.0001$.

distinct populations of differentiated and de-differentiated PT cells in $GC^{ER}RAR\alpha\Delta$ mice. Co-staining of CCL2 with Ki67 revealed that 52% of the proliferating cells in $GC^{ER}RAR\alpha\Delta$ cortices 3 d post-tam were de-differentiated PTs (*SI Appendix*, Figs. S9 and S11), indicating that PTs were undergoing repair.

We sought to discern whether PTs in the repair cycle were RARα positive or negative and observed that the majority of CCL2+ tubules were RARα negative in $GC^{ER}RAR\alpha\Delta$ mice 3 d post-tam (*SI Appendix*, Fig. S12). Collectively, these data suggest the surviving PTs of $GC^{ER}RAR\alpha\Delta$ mice enter a tubular repair pathway in response to injury caused by RARα deletion.

The Deletion of RARα in PTs Leads to Mitochondrial Distress. We next aimed to understand how RARα deletion was causing PT injury, as indicated by apoptosis. One of the numerous signaling pathways involved in apoptosis is oxidative stress, which can be detected through an increase in the lipid peroxidation product 4-hydroxy-2-nonenal (4HNE) (32, 33). We observed a 6.1-fold ($P < 0.0001$) increase in 4HNE level in $GC^{ER}RAR\alpha\Delta$ mice 3 d post-tam compared to WT (Fig. 2 *G* and *H*), suggesting that oxidative stress is one of the initial responses to RARα deletion in PTs. This increase in oxidative stress at 3 d post-tam is seen only in females (*SI Appendix*, Figs. S13 and S14). In cases of AKI, the autophagy pathway, assessed here by expression of autophagy related 7 (ATG7), prevents accumulation of damaged organelles and degeneration of PTs (34, 35). Dysfunctional mitochondria, which have impaired degradation of PTEN-induced kinase 1 (PINK1), are removed via mitophagy, a selective form of autophagy (36). We observed 4.4-fold ($P < 0.0001$) and 1.4-fold ($P < 0.01$) increases in ATG7 and PINK1, respectively, in PTs of $GC^{ER}RAR\alpha\Delta$ mice 3 d post-tam compared to WT (Fig. 2 *I–K*). These increases at 3 d post-tam were followed by a 1.7-fold ($P < 0.05$) decrease of ATG7 and a 1.3-fold ($P < 0.05$) decrease of PINK1 in PTs of $GC^{ER}RAR\alpha\Delta$ mice at 3 mo post-tam. Interestingly, we noted that the majority of ATG7+ cells also expressed PINK1 in $GC^{ER}RAR\alpha\Delta$ kidneys (Fig. 2*I*, *black arrows*), indicating that autophagy was specific to PT cells with damaged mitochondria.

RARα Expression Maintains Mitochondrial Structural Integrity in PT Cells. To further investigate the role of RARα in mitochondrial health, we evaluated $GC^{ER}RAR\alpha\Delta$ PTs at a higher magnification utilizing transmission electron microscopy (TEM). We observed increased spaces between microvilli (Fig. 3*A*, *yellow arrows*), indicating brush border loss, massively swollen mitochondria with disrupted inner membrane folding (cristae) (Fig. 3*A*, *black asterisks*), and accumulation of RNA granules appearing on mitochondria (Fig. 3*A, white arrows*), which collectively indicate tubule injury and major mitochondrial damage (37, 38). In contrast, mitochondria of WT PT cells showed normal mitochondrial morphology (Fig. 3*A*, *blue asterisks*). Further analysis indicated that mitochondria of $GC^{ER}RAR\alpha\Delta$ mice 4.5 mo post-tam were 2.9-fold ($P < 0.0001$) larger (Fig. 3*B*), with a twofold ($P < 0.0001$) decreased cristae volume density (Fig. 3*C*), compared to age-matched WT. These data show that RARα expression in PTs contributes to the structural integrity of mitochondria.

Cristae structure is important for energy production of the mitochondria because it is the location of the electron transport respiratory complexes (I-V), which generate ATP through oxidative phosphorylation (39). Swelling of the mitochondria and cristae disruption have been correlated with respiratory complex deficiencies, particularly of complex I in kidney pathologies (40, 41). Complex I consists of at least 44 subunits and 14 assembly factors and mutations in any of these proteins can cause complex I deficiency (42). We observed that mRNA levels of NDUFA1, a crucial component of complex I assembly (43), were decreased 17.8% ($P < 0.01$) in kidney cortices of $GC^{ER}RAR\alpha\Delta$ mice 3 d post-tam compared to WT (Fig. 3*D*). Collectively, these data suggest that one of the mechanisms by which RARα deletion in PTs leads to mitochondrial damage is by affecting complex I assembly.

To further investigate whether RARα deletion and decreased NDUFA1 reduce mitochondrial function, we utilized an immortalized PT cell line (HK-2) (44) with a CRISPR/Cas9 KO of RARα (*SI Appendix*, Fig. S15). This cell line allowed us to observe mitochondrial activity in real time while avoiding measuring the effects of other cell types in cortical tissue. Additionally, the HK-2 RARα KO cells had a 20% decrease in complex I protein NDUFB8 level, when compared to HK-2 parental control cells (*SI Appendix*, Fig. S16), showing that RARα deletion also reduces the expression of complex I components in our in-vitro model. We utilized a Seahorse Extracellular Flux (XFe96) Analyzer to test for mitochondrial stress and observe mitochondrial activity and energetics (*SI Appendix*, Fig. S17). Compared to HK-2 parental cells, the HK-2 RARα KO cells had a 40.7% ($P < 0.0001$) lower basal respiration rate (*SI Appendix*, Fig. S18). We next evaluated spare capacity, which indicates the cell's adaptability to stress or changes in energy demand, as decreases in spare capacity may indicate decreased structural and/or ETC integrity of the mitochondria (45), and we detected a 47.8% ($P < 0.0001$) decrease in spare capacity in HK-2 RARα KO cells vs. HK-2 parental cells (*SI Appendix*, Fig. S19). Our data indicate that loss of RARα in PT cells decreases mitochondrial function and energetics.

PT-Specific Loss of RARα Leads to Prolonged Kidney Injury and Development of CKD. We next assessed the long-term effects of RARα deletion on PT cells. Kidney injury and/or dysfunction lasting 3 or more months is considered chronic (1); therefore, we chose 3- and 4.5-mo time points post-tam to evaluate the prolonged effects of RARα KO in PTs. We observed a twofold ($P < 0.01$) decrease in LTL (11) staining in $GC^{ER}RAR\alpha\Delta$ males vs. $GC^{ER}RAR\alpha^{fl/fl}$ males at 2 mo post-tam; there was no significant change between female groups (Fig. 4 *A* and *B*). By 3 mo post-tam, we detected a 3.6-fold ($P < 0.0001$) decrease of LTL expression in male $GC^{ER}RAR\alpha\Delta$ vs. $GC^{ER}RAR\alpha^{fl/fl}$ mice and a 2.4-fold decrease ($P < 0.0001$) in LTL expression in female $GC^{ER}RAR\alpha\Delta$ vs. $GC^{ER}RAR\alpha^{fl/fl}$ mice (Fig. 4*C*). While both male and female $GC^{ER}RAR\alpha\Delta$ mice showed a decrease in LTL+ tubules, $GC^{ER}RAR\alpha\Delta$ females additionally displayed increases of interstitial spaces between LTL+ tubules over time. The expression of kidney injury molecule-1 (KIM-1), a transmembrane glycoprotein also known as hepatitis A virus cellular receptor 1, greatly increases in PT cells after kidney injury (46). We observed a 11.9-fold ($P < 0.0001$) increase in KIM-I in PT cells of $GC^{ER}RAR\alpha\Delta$ mice 3 mo post-tam vs. WT (Fig. 4 *D* and *E*). Prolonged tubular injury is often associated with a loss of brush border and vacuolization of PT epithelium (47–49). We detected evidence of brush border loss (Fig. 4*F*, *black arrows*) in PTs of $GC^{ER}RAR\alpha\Delta$ females 3 mo post-tam by utilizing a periodic acid–Schiff (PAS) stain to accentuate matrix and basement membrane constituents (50). In contrast, brush border remained intact in WT. Thus, RARα deletion in PTs of adult mice is sufficient to cause prolonged kidney injury.

The Deletion of RARα in PTs Does Not Cause Injury in the Glomeruli or Distal Tubules. To determine whether PT-specific RARα deletion caused injury in additional renal cell types, we examined neighboring cortical cells. We measured the sizes of glomeruli in the kidney cortices previously stained with PAS and did not note any changes in glomerular sizes in WT compared to $GC^{ER}RAR\alpha\Delta$ mice 3 mo post-tam (Fig. 4 *G* and *H*). We also

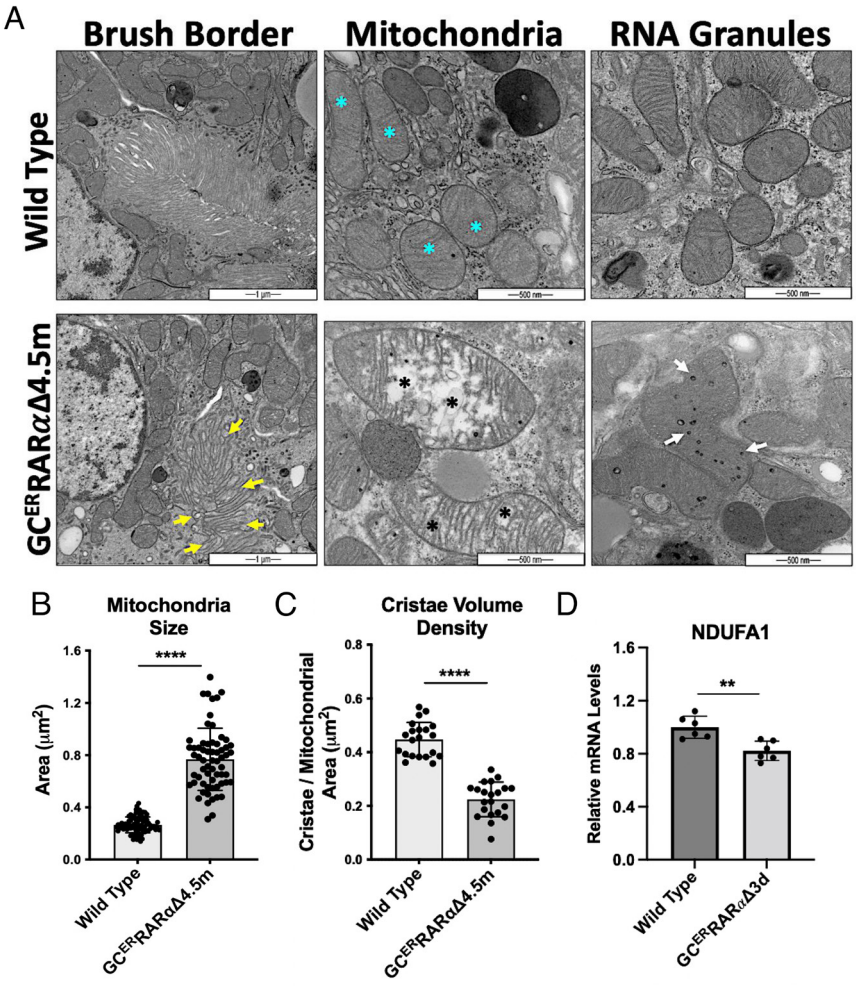

Fig. 3. RARα expression maintains mitochondrial integrity and function in PT cells. (*A*) Representative images (15 fields/mouse) of TEM of GC^{ER}RARαΔ females 4.5 mo post-tamoxifen and age-matched wild-type females (n = 3/group). (*B*) Quantification of mitochondrial size (μm^2) (n = 26 mitochondria/group). (*C*) Quantification of cristae volume density (μm^2) calculated by dividing the total area of cristae per mitochondria by the total area of mitochondria (n = 7 mitochondria/group). (*D*) Relative mRNA levels by qRT-PCR of NDUFA1 from kidney cortices of GC^{ER}RARαΔ females 3 d post-tam and age-matched wild-type females (n = 6/group). TEM magnification at 20,000× (1 μm scale bar) for brush border images and 50,000× (500 nm scale bar) for mitochondria and RNA granule images (*A*). $^{**}P < 0.01$ and $^{****}P < 0.0001$.

did not detect changes in the percentages of cells stained with E-cadherin, a distal tubule marker (51), in GC^{ER}RARαΔ 3 mo post-tam vs. GC^{ER}RARα$^{fl/fl}$ mice (Fig. 4 *I* and *J*). These data indicate that PT cells are injured in GC^{ER}RARαΔ mice without apparent injury to other cortical cell types, such as the distal tubules and glomeruli.

Loss of RARα in PTs Leads to an Increase in TGF-β1 Expression and Interstitial Fibrosis. Prolonged PT injury causes the secretion of profibrotic factors, such as TGF-β1, which activate myofibroblasts and initiate fibrosis, resulting in the transition from AKI to CKD (10, 13, 48, 52). We noted a 29.3-fold ($P < 0.0001$) increase in TGF-β1 levels in PT cells from GC^{ER}RARαΔ females 3 mo post-tam relative to WT (Fig. 5 *A* and *B*). Additionally, TGF-β1 overlapped with GGT1-stained PTs, indicating that TGF-β1 was secreted from PT cells targeted by the GGT1-CreER. There was no difference in TGF-β1 levels between GC^{ER}RARαΔ males 3 mo post-tam compared to WT (*SI Appendix*, Figs. S20 and S21); however, both male and female GC^{ER}RARαΔ mice displayed increased TGF-β1 expression 3 d post-tam when compared to WT controls (*SI Appendix*, Figs. S20 and S21). Therefore, although both males and females have increased TGF-β1 expression/secretion initially after PT-specific deletion of RARα, this phenotype only persists long-term (3 mo) in females. Although TGF-β1 can regulate several cellular pathways, TGF-β1/Smad signaling, specifically through phosphorylation/activation of Smads 2 and 3, contributes to fibrosis and inflammation in the context of renal injury (52–55). We observed a 5.0-fold ($P < 0.0001$) increase in phosphorylated Smad3 (p-Smad3) in kidney cortices of GC^{ER}RARαΔ mice 3 mo post-tam vs. WT (Fig. 5 *C* and *D*).

We next assessed interstitial fibrosis and observed 1.7-fold ($P < 0.0001$), and 1.5-fold ($P < 0.001$) increases in collagen deposition in kidney cortices of GC^{ER}RARαΔ males and females, respectively, 3 mo post-tam compared to age-matched WT (Fig. 5 *E* and *F*). There was no further progression of fibrosis in male GC^{ER}RARαΔ mice at 4.5 mo post-tam. However, collagen deposition in GC^{ER}RARαΔ females increased an additional 1.5-fold ($P < 0.0001$) between the 3-mo and 4.5-mo post-tam time points. These findings show that interstitial fibrosis develops in GC^{ER}RARαΔ mice and becomes progressively worse in females. We do not yet understand why females have a worse fibrotic phenotype; however, sex hormones may have sexually dimorphic effects on RA signaling (56).

We then determined which cell types contributed to the development of tubulointerstitial fibrosis. Prolonged TGF-β1 secretion prompts residential fibroblasts to trans-differentiate into

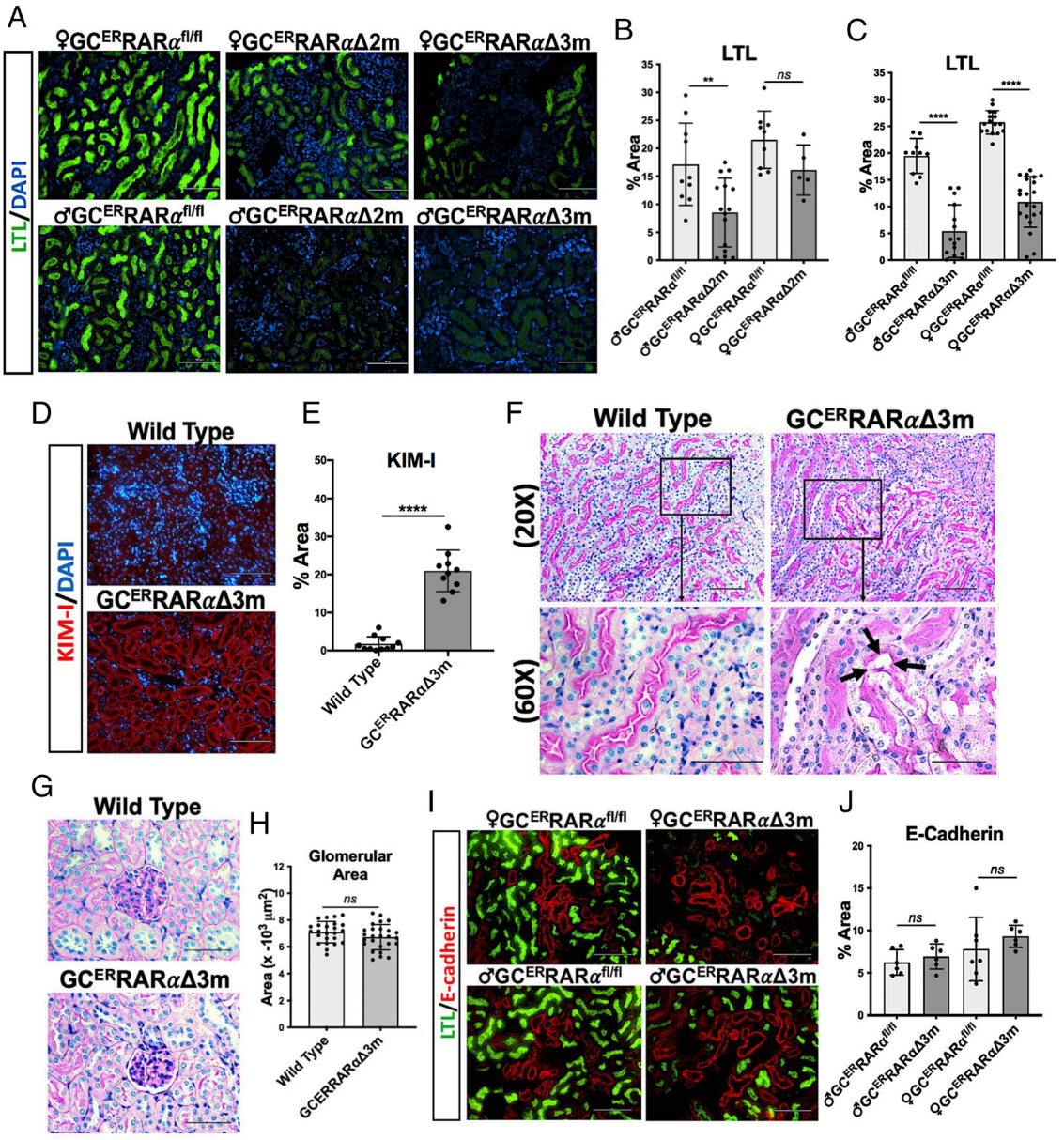

Fig. 4. PT-specific deletion of RARα leads to prolonged kidney injury and development of CKD. (*A*) Representative images of LTL-stained kidney cortices from GC^{ER}RARαΔ males and females 2 mo post-tamoxifen and 3 mo post-tamoxifen (n = 3/group), and GC^{ER}RARα$^{fl/fl}$ males and females (n = 3/group) age-matched to the GC^{ER}RARαΔ 3-mo post-tamoxifen group. (*B*) Quantification of LTL % area fluorescence of 2-mo groups. (*C*) Quantification of LTL % area fluorescence of 3-mo groups. (*D*) Representative images (3 to 5 fields/mouse) of kidney injury molecule-I (KIM-I)-stained kidney cortices from GC^{ER}RARαΔ females 3 mo post-tamoxifen and age-matched wild-type females (n = 3/group). (*E*) Quantification of KIM-I % area fluorescence. (*F*) Representative images (8 fields/mouse) of PAS-stained female mice described in (*D*) highlighting PT brush border. (*G*) Additional representative images of PAS-stained sections from (*F*) focusing on glomeruli (n = 3/group). (*H*) Quantification of glomerular area (μm^2) (n = 25 glomeruli/group). (*I*) Representative images (3 fields/mouse) of LTL (GFP) and E-cadherin (TXRED) co-stained kidney cortices from GC^{ER}RARαΔ males and females 3 mo post-tamoxifen (n = 3/group) and age-matched GC^{ER}RARα$^{fl/fl}$ males and females (n = 3/group). (*J*) Quantification of E-cadherin % area fluorescence. Magnification 200× (*A*, *D*, *F*, and *I*) with a 100-μm scale bar or 600× (*F* and *G*) with a 50-μm scale bar. Error bars represent SD. ****$P < 0.0001$.

myofibroblasts (10, 48, 57). Additionally, prolonged inflammation in response to PT injury is another source of growth factor secretion and myofibroblast activation (8). We observed a 2.6-fold ($P < 0.0001$) increase in the expression of alpha smooth muscle actin (α-SMA), a marker of activated myofibroblasts (58) (Fig. 5 *G* and *H*), and a 2.3-fold ($P < 0.0001$) increase in F4/80, a macrophage marker (12) (Fig. 5 *I* and *J*), in kidney cortices of GC^{ER}RARαΔ females 3 mo post-tam relative to WT. These results indicate that prolonged PT injury post-deletion of RARα leads to tubulointerstitial fibrosis via inflammatory cell infiltration, TGF-β1 secretion from injured PTs, and myofibroblast activation. The overall short and long-term effects of PT-specific RARα are summarized in (Fig. 6).

Retinoid Levels Are Altered after RARα Loss in PTs. Retinoid metabolism is known to be altered in a variety of kidney diseases (20, 59). Utilizing liquid chromatography-mass spectrometry (LC-MS) and retinoid standards (*SI Appendix*, Fig. S22), we examined retinoid levels in sera and kidney cortices of wild-type and GC^{ER}RARαΔ females at early (3 d post-tam) and later (3 mo post-tam) time points. Compared to WT, the sera of GC^{ER}RARαΔ females 3 d post-tam displayed a 1.9-fold

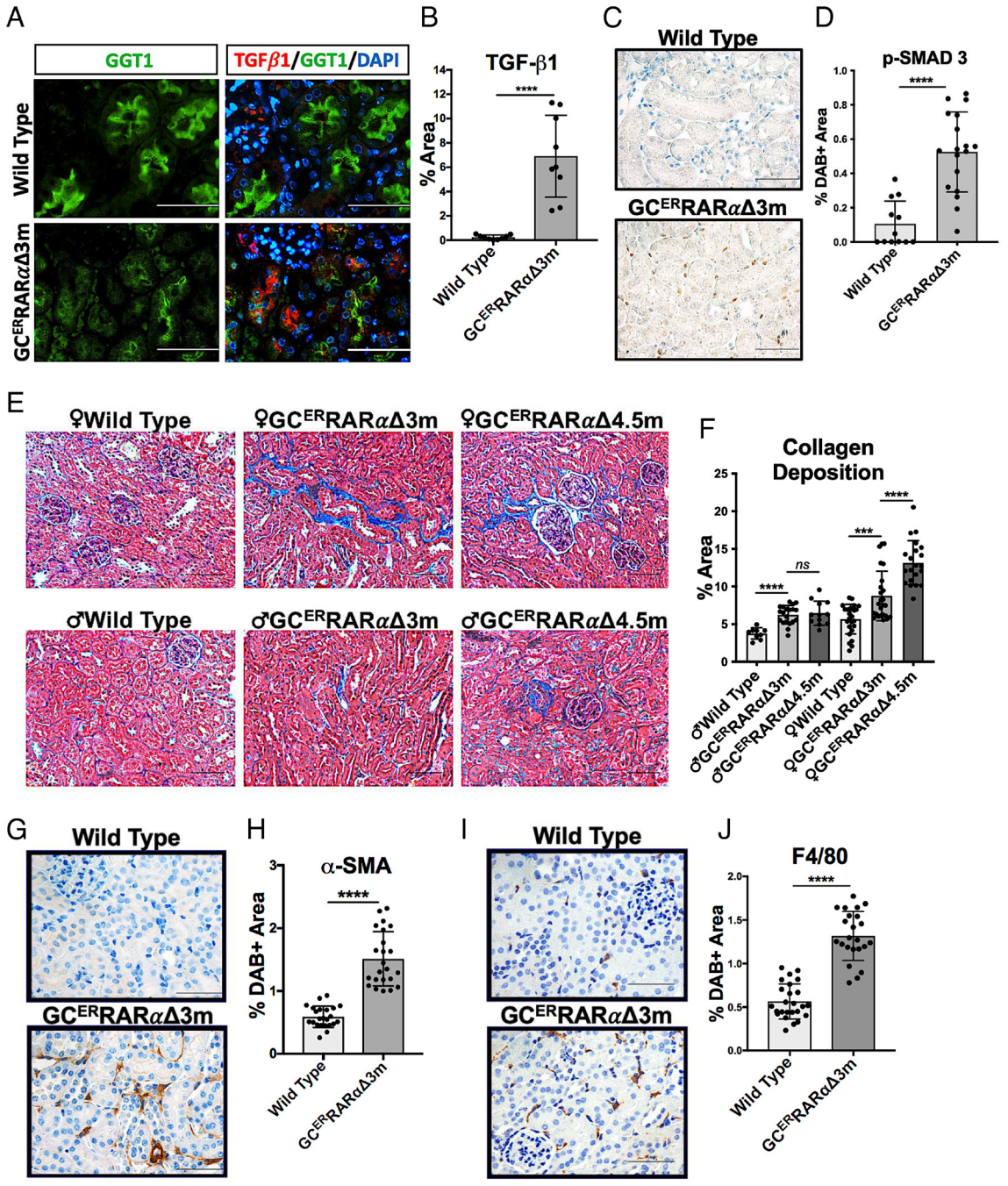

Fig. 5. Loss of RARα in PTs leads to an increase in TGF-β1 expression and interstitial fibrosis. (*A*) Representative images (3 fields/mouse) of LTL (GFP) and TGF-β1(TXRED) co-stained kidney cortices from GC^{ER}RARαΔ females 3 mo post-tamoxifen and age-matched wild-type females (n = 3/group). (*B*) Quantification of TGF-β1 % area fluorescence. (*C*) Representative images (4 to 6 fields/mouse) of p-SMAD3-stained kidney cortices from mice described in (*A*). (*D*) Quantification of p-SMAD3+ % area. (*E*) Representative images (3 to 6 fields/mouse) of Masson's Trichrome-stained kidney cortices from GC^{ER}RARαΔ males and females 3 mo and 4.5 mo post-tamoxifen (n = 4/group) and wild-type males and females (n = 3/group) age-matched to the GC^{ER}RARαΔ 4.5 mo post-tamoxifen group. (*F*) Quantification of % area of collagen (blue). (*G*) Representative images (7 to 8 fields/mouse) of α-SMA-stained kidney cortices from mice described in (*A*). (*H*) Quantification of α-SMA+ % area. (*I*) Representative images (7 to 8 fields/mouse) of F4/80-stained kidney cortices of mice described in (*A*). (*J*) Quantification of F4/80+ % area. Magnification 200× (*E*) with a 100-μm scale bar or 600× (*A*, *C*, *G*, and *I*) with a 50-μm scale bar. Error bars represent SD. ***$P < 0.001$ and ****$P < 0.0001$.

($P < 0.05$) increase in retinol (ROL) and a 1.4-fold ($P < 0.05$) decrease in retinyl palmitate (RP), without any significant changes in RA levels, although there was more variation in RA levels among the mice as compared to ROL and RP most likely due to small sample size (*SI Appendix*, Fig. S23). In contrast, we did not detect differences in ROL, RP, or RA levels between GC^{ER}RARαΔ females 3 d post-tam and WT in kidney cortices (*SI Appendix*, Fig. S24).

Sera from GC^{ER}RARαΔ females 3 mo post-tam did not display any significant changes in levels of ROL, RP, or RA compared to WT (*SI Appendix*, Fig. S23). However, we observed a 1.5-fold ($P < 0.01$) decrease in ROL, a 1.4-fold ($P < 0.05$) decrease in RA, and a 1.6 ($P < 0.05$) increase in RP in the kidney cortices of GC^{ER}RARαΔ females 3 mo post-tam vs. WT (*SI Appendix*, Fig. S24). These data show that some retinoid levels are altered in sera of GC^{ER}RARαΔ females 3 d post-tam and kidney cortices of

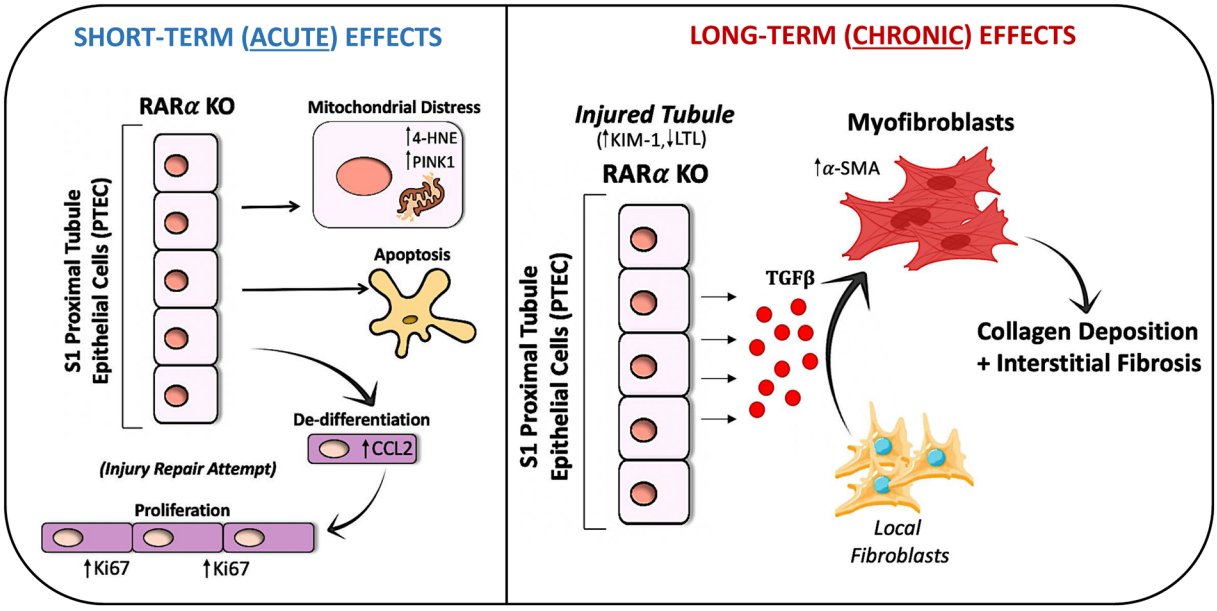

Fig. 6. Model of the short- and long-term effects of PT-specific RARα KO. Short-term (acute/3 d post-tam) effects of RARα loss in segment 1 (S1) of PTs are mitochondrial distress, autophagy, mitophagy, and apoptosis. Surviving RARα negative PT cells enter a repair cycle during which they de-differentiate and proliferate to replace injured PT cells. However, RARα loss is sufficient to cause prolonged (chronic/>3 mo post-tam) injury without any external stimuli. Injured S1 PT cells secrete TGF-β1, activating residential fibroblasts to myofibroblasts and leading to ECM deposition and interstitial fibrosis.

GC^{ER}RARαΔ females 3 mo post-tam, and that these changes are inversely related. Collectively, we observed that RARα loss in PTs affects retinoid levels in mouse kidneys and sera.

RARα Deletion in PTs Impairs Kidney Function without Impacting Glycemic Control. Kidney injury is first diagnosed through a variety of serum and urine tests that determine kidney functionality (60). Elevated serum biomarkers, such as creatinine and blood urea nitrogen (BUN), are indicators of kidney dysfunction (61, 62). Both males and females showed no significant changes in serum creatinine levels between WT and GC^{ER}RARαΔ mice at either 3 d or 3 mo post-tam (Fig. 7 *A* and *B*). At 4.5 mo post-tam there were still no significant changes in serum creatinine between male groups; however, female GC^{ER}RARαΔ mice showed a 26.6% ($P < 0.001$) increase in serum creatinine levels (Fig. 7*C*), indicating impaired kidney function. Similarly, at 3 d post-tam, there were no significant changes in BUN levels between WT and GC^{ER}RARαΔ males or females (Fig. 7*D*). However, at 3 mo post-tam, GC^{ER}RARαΔ males displayed a 31.4% ($P < 0.05$) increase in BUN while GC^{ER}RARαΔ females displayed a 30.6% ($P < 0.05$) increase in BUN relative to WT (Fig. 7*E*). Collectively, these data indicate that loss of RARα in PTs of GC^{ER}RARαΔ mice is sufficient to have negative, long-term effects on kidney function, with a more significant impact on females. We additionally looked at BUN levels in WT mice that were killed 3 d after tamoxifen treatment to discern whether tamoxifen affected kidney function and we did not see any significant differences between groups (*SI Appendix*, Fig. S25).

β2-microglobulin (β2m) is a biomarker that indicates glomerular damage when elevated in serum and PT damage when elevated in urine (63). As expected, we observed no significant changes in β2m levels in GC^{ER}RARαΔ sera at 4.5 mo post-tam (Fig. 7*F*), suggesting that impaired kidney function in GC^{ER}RARαΔ mice does not result from glomerular pathology. We then measured β2m levels in urine and normalized these values to urine creatinine levels (UβCR). At 4.5 mo post-tam, we detected an 82.1% ($P < 0.01$) increase and a 64.9% ($P < 0.01$) increase in the UβCR of GC^{ER}RARαΔ males and females relative to WT, respectively (Fig. 7*G*). These elevated UβCRs indicate that impaired kidney function of GC^{ER}RARαΔ mice results from PT injury. Although GC^{ER}RARαΔ mice show evidence of renal dysfunction, we did not detect hyperglycemia (*SI Appendix*, Fig. S26), indicating that the kidney injury does not change glucose regulation in other tissues, such as the liver or pancreas.

Discussion

RA, an agonist of the three RARs (α, β, and γ), has several functions in embryonic development, including the regulation of genes essential for stem cell differentiation (17). Low levels of maternal vitamin A (retinol, VA) and/or variants of enzymes that convert VA to RA contribute to RA deficiency in the fetus, which in turn disrupts renal morphogenesis and causes a reduction in the number of embryonic nephrons (18, 64). RA receptors α and β are vital for kidney morphogenesis as they regulate the expression of c-ret, a protein required for ureteric bud branching (21). However, the functions of the RARs in the adult kidney have not been well defined to date. We show here that RARα is required for PT survival in adult mice. Our study also further defines the roles of RARα in PTs. We show that loss of RARα in PTs results in prolonged kidney injury and subsequent interstitial fibrosis, similar to the development and progression of AKI to CKD in humans.

Kidney PT cells are highly metabolically active and thus contain more mitochondria than any other renal cell type (65). Mitochondrial homeostasis can be modulated by RA and damage/dysfunction of mitochondria plays a critical role in kidney injury and progression to CKD (66–68). Tran et al. observed swollen and enlarged tubular mitochondria in a mouse model of AKI (69). We also see this phenotype in our mouse model; 4.5 mo after RARα deletion, mitochondria from the PTs are overtly enlarged and have a lower volume density of cristae (37, 38). Additionally, loss of in RARα expression in PTs leads to oxidative stress and impacts mitochondrial energetics. Loss of cristae structure highly impacts mitochondrial function due to decreased electron transport chain activity. Renal Fanconi Syndrome is a proximal tubular

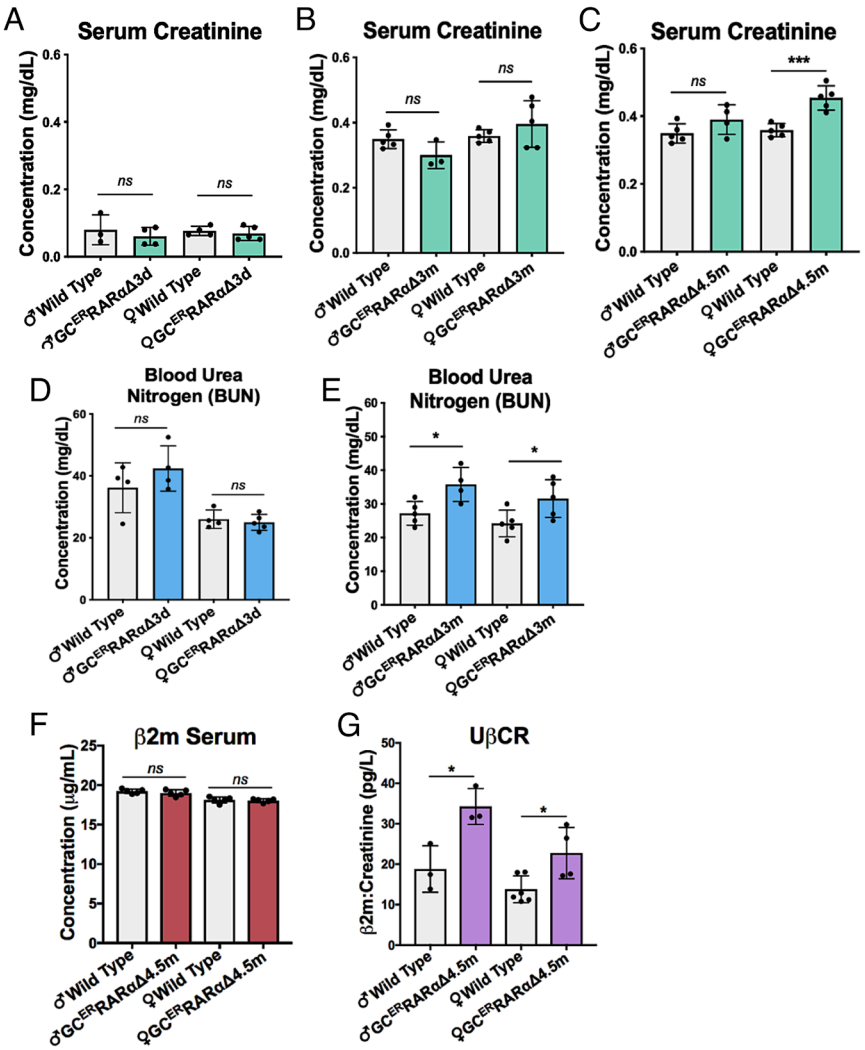

Fig. 7. RARα deletion in PTs leads to impaired kidney function without impacting glycemic control. (*A*) Serum Creatinine (mg/dL) of GC^{ER}RARαΔ males (n = 4) and females (n = 5) 3 d post-tamoxifen and age-matched wild-type males (n = 3) and females (n = 4). (*B*) Serum Creatinine (mg/dL) of GC^{ER}RARαΔ males (n = 3) and females (n = 5) 3 mo post-tamoxifen and age-matched wild-type males and females (n = 5/group). (*C*) Serum Creatinine (mg/dL) of GC^{ER}RARαΔ males (n = 4) and females (n = 5) 4.5 mo post-tamoxifen and age-matched wild-type males and females (n = 5/group). (*D*) BUN (mg/dL) of GC^{ER}RARαΔ males (n = 4) and females (n = 5) 3 d post-tamoxifen and age-matched wild-type males and females (n = 4/group). (*E*) BUN (mg/dL) of GC^{ER}RARαΔ males (n = 4) and females (n = 5) 3 mo post-tamoxifen and age-matched wild-type males and females (n = 5/group). (*F*) β2m of serum (μg/mL) from GC^{ER}RARαΔ males and females 4.5 mo post-tamoxifen (n = 5/group) and age-matched wild-type males and females (n = 5/group). (*G*) Urine β2m (pg/L) to creatinine (pg/L) ratio (UβCR) of GC^{ER}RARαΔ males (n = 3) and females (n = 4) 4.5 mo post-tamoxifen and age-matched wild-type males (n = 3) and females (n = 6). Error bars represent SD. *P < 0.05 and ***P < 0.001.

defect that causes prolonged kidney injury and progressive loss of renal structure and function (70), similar to what we have observed in our model. There are several causes of Renal Fanconi Syndrome, but one cause is a mutation in an assembly factor of respiratory complex I (NDUFAF6), which leads to enlarged and damaged mitochondria (70). We saw that the mRNA levels of NDUFA1, another crucial component of complex I assembly (43), were reduced in our PT-specific KO mice, indicating that RARα may regulate some of the critical genes for respiratory complex I assembly in PT cells.

Mitophagy occurs frequently in response to mitochondrial dysfunction to lower the impact of oxidative stress (69). Notably, we see an early increase (3 d post-tam) in tubule mitophagy, as assessed by higher levels of PINK1, in kidney cortices of the PT-specific RARα KO compared to WT mice, a majority of which overlap with cells undergoing autophagy. Additionally, we observed increases in apoptosis, de-differentiation, and proliferation, all of which are signaling pathways known to be regulated by RARs (19, 71, 72). The concurrent increases of these pathways in RARα negative PT cells indicate that PTs enter a repair pathway after the deletion of RARα. This repair pathway is a common response seen in cases of AKI (11, 28). However, prolonged injury and inflammation may lead to maladaptive repair and progressive fibrosis (9, 73).

Bhatia et al. report that mitochondrial dysfunction is correlated with prolonged inflammation and the conversion of AKI to CKD (67, 74). We see a significant increase in inflammation in the cortices of PT-RARα KO mice at a later time-point (3 mo post-tam). Both inflammation and maladaptive repair cause interstitial fibrosis by increasing transforming growth factor β (TGF-β1) secretion, which then activates collagen-producing myofibroblasts and ECM deposition (10, 75). We observed these prolonged effects in our PT-RARα KO mice, indicating that KO of RARα in PTs causes long-term injury and mimics progression to CKD without the addition of any external injury stimuli. Collectively, these results allow us to identify a major role for RARα in maintaining PT homeostasis.

Although in most experiments we did not perform tamoxifen (tam) treatments on WT mice, researchers have shown that tam

treatment does not affect the extent of kidney injury in an ischemia-reperfusion kidney injury murine model even as the acute injury turned into CKD (76). We also showed that the tam-treatment did not impact kidney functionality in WT mice, as evaluated by BUN levels. Thus, we would not anticipate any effects of tam on the kidney in WT mice.

Disruptions in vitamin A levels are found in some renal diseases (59, 77). Several studies have shown increased plasma concentrations of retinol binding protein 4, retinol, and RA in humans with CKD (20). Our data show that early (3 d) after RARα deletion in PTs there is an increase in serum ROL mirroring that seen in CKD (20). Conversely, RA levels are decreased in diabetic kidney cortices and livers (59). We found that RA levels are decreased in kidney cortices 3 mo after deletion of RARα in PTs. Our research suggests that the decreases in RA levels in kidney diseases cause reductions in RARα activity, leading to mitochondrial dysfunction, apoptosis, and failed PT repair.

Interestingly, many of the phenotypes observed in the PT-specific RARα, such as proliferation, oxidative stress, and fibrosis, were more severe in females. Sex hormones have been reported to have sexually dimorphic effects on RA signaling; estrogen increases RA biosynthesis and induces RARβ, while androgens repress RARα and RARγ (56). The higher expression levels of RARα and RA signaling in females may be contributing to the stronger phenotypes we observed in PT-specific RARα KO females. However, further investigation will be needed to determine the root cause of these sexually dimorphic phenotypes. In a human setting, women are also more prone than men to develop CKD (14 vs. 12%), but this difference is suspected to be due to the increased likelihood of injury by urinary tract infections in women (78).

Numerous studies have demonstrated beneficial effects of RA administration in the treatment of kidney diseases (14). RA can ameliorate progressive renal fibrosis in mice that underwent unilateral ureteral obstruction (UUO) surgery, as well as decrease the severity of fibrosis when administered prior to UUO (79, 80). Sierra-Mondragon et al. showed that RARα expression is inversely related to tubulointerstitial fibrosis; RARα was decreased in a DN mouse model and RA administration restored RARα levels and decreased fibrosis (22). RAR-selective agonists have also been studied. Our lab has previously shown that administration of AC261066, a RARβ2 agonist, ameliorates DN in a mouse model (81). Other groups have reported the protective effects of Am580 and other RARα agonists in renal injury (82, 83). Our PT-specific KO of RARα not only demonstrates the importance of RARα in maintaining PT homeostasis but also provides a mouse model for further investigation of injury and fibrosis in the context of kidney diseases.

Materials and Methods

Animals. Equal numbers of male and female mice on a standard laboratory chow diet (13% kcal fat, no. 5053; Pico Diet, St. Louis, MO) were utilized. The model used for this study is a transgenic PT-specific RARα KO mouse on a C57BL/6 background and was generated by crossing floxed RARα mice (from Pierre Chambon) (25) with a transgenic line generated in the Gudas lab to express a tamoxifen-dependent Cre recombinase (CreER) driven by a truncated GGT1 promoter (23). This construct is expressed almost exclusively in segment 1 of the proximal convoluted tubules of the kidney (24, 84). Details on genotyping, experimental, conditions, group randomization, and analysis of RARα KO efficiency are in *SI Appendix*.

Serum/Urine Analyses and Glucose Tolerance Tests. Details of these analyses are in *SI Appendix*.

Immunohistochemical Assays and Antibodies. Details are in *SI Appendix*.

TEM. Tissue was placed in fixative obtained from Weill Cornell Histology Core (2.5% glutaraldehyde, 4% paraformaldehyde, and 0.02% picric acid in 0.1M sodium cacodylate buffer, pH 7.3) overnight at 4 °C. TEM was then performed by personnel at the Microscopy and Imaging Core Facility at Weill Cornell Medical College.

Generation of RARα KO Cell Line and Seahorse Analytics. Details are in *SI Appendix*

General Metabolomics. Details for Metabolite extraction are in *SI Appendix*. Further information for Q-TOF LC/MS Data Acquisition and Analysis of extracted metabolites is detailed in the attached ref. 85.

Statistics. Immunofluorescent and immunohistochemical images were quantified using Image J (detailed in *SI Appendix*). All statistical analyses were performed using unpaired parametric *t* tests in GraphPad Prism and are reported as mean ± SD with significant differences defined as *P*-values less than an alpha of 0.05 (*$P < 0.05$, **$P < 0.01$, ***$P < 0.001$, and ****$P < 0.0001$).

Study Approval. The use of animals was approved by the Resource Animal Research Center at Weill Cornell Medicine, protocol 0705-615A.

Data, Materials, and Software Availability. The data obtained in this study will be accessible at the NIH Common Fund's NMDR, the Metabolomics Workbench, https://www.metabolomicsworkbench.org (86).

ACKNOWLEDGMENTS. This work was supported through the following grants: NIH R01DK113088 (L.J.G.) and NCI T32 (5T32CA062948-26). We thank Gudas and Choi lab members for helpful discussions and critically reading this manuscript before submission, personnel at the Microscopy and Imaging Core Facility at Weill Cornell Medical College for taking TEM images, and Dr. Jianjun Xie for submission of the manuscript.

1. A. S. Levey, C. Becker, L. A. Inker, Glomerular filtration rate and albuminuria for detection and staging of acute and chronic kidney disease in adults: A systematic review. *JAMA* **313**, 837–846 (2015).
2. A. C. Webster, E. V. Nagler, R. L. Morton, P. Masson, Chronic kidney disease. *Lancet* **389**, 1238–1252 (2017).
3. K. L. Cavanaugh, Diabetes management issues for patients with chronic kidney disease. *Clin. Diabetes* **25**, 90–97 (2007).
4. S. Said, G. T. Hernandez, The link between chronic kidney disease and cardiovascular disease. *J. Nephropathol.* **3**, 99–104 (2014).
5. D. Alfego *et al.*, Chronic kidney disease testing among at-risk adults in the U.S. remains low: Real-world evidence from a National Laboratory Database. *Diabetes Care* **44**, 2025–2032 (2021).
6. K. C. Leung, M. Tonelli, M. T. James, Chronic kidney disease following acute kidney injury-risk and outcomes. *Nat. Rev. Nephrol.* **9**, 77–85 (2013).
7. K. Takaori *et al.*, Severity and frequency of proximal tubule injury determines renal prognosis. *J. Am. Soc. Nephrol.* **27**, 2393–2406 (2016).
8. Y. Liu, Cellular and molecular mechanisms of renal fibrosis. *Nat. Rev. Nephrol.* **7**, 684–696 (2011).
9. H. Li, E. E. Dixon, H. Wu, B. D. Humphreys, Comprehensive single-cell transcriptional profiling defines shared and unique epithelial injury responses during kidney fibrosis. *Cell Metab.* **34**, 1977–1998.e9 (2022).
10. T. A. Wynn, Fibrosis under arrest. *Nat. Med.* **16**, 523–525 (2010).
11. T. Kusaba, M. Lalli, R. Kramann, A. Kobayashi, B. D. Humphreys, Differentiated kidney epithelial cells repair injured proximal tubule. *Proc. Natl. Acad. Sci. U.S.A.* **111**, 1527–1532 (2014).
12. S. Van Linthout, K. Miteva, C. Tschöpe, Crosstalk between fibroblasts and inflammatory cells. *Cardiovasc. Res.* **102**, 258–269 (2014).
13. F. Strutz, M. Zeisberg, Renal fibroblasts and myofibroblasts in chronic kidney disease. *J. Am. Soc. Nephrol.* **17**, 2992 (2006).
14. K. M. DiKun, L. J. Gudas, Vitamin A and retinoid signaling in the kidneys. *Pharmacol. Ther.* **248**, 108481 (2023).
15. O. V. Belyaeva, M. K. Adams, K. M. Popov, N. Y. Kedishvili, Generation of retinaldehyde for retinoic acid biosynthesis. *Biomolecules* **10**, 5 (2019).
16. L. J. Gudas, Synthetic retinoids beyond cancer therapy. *Annu. Rev. Pharmacol. Toxicol.* **62**, 155–175 (2021), 10.1146/annurev-pharmtox-052120-104428.
17. L. J. Gudas, J. A. Wagner, Retinoids regulate stem cell differentiation. *J. Cell Physiol.* **226**, 322–330 (2011).
18. M. Lelièvre-Pégorier *et al.*, Mild vitamin A deficiency leads to inborn nephron deficit in the rat. *Kidney Int.* **54**, 1455–1462 (1998).
19. J. Nakamura *et al.*, Myofibroblasts acquire retinoic acid-producing ability during fibroblast-to-myofibroblast transition following kidney injury. *Kidney Int.* **95**, 526–539 (2019).
20. J. Jing *et al.*, Chronic kidney disease alters vitamin A homeostasis via effects on hepatic RBP4 protein expression and metabolic enzymes. *Clin. Transl. Sci.* **9**, 207–215 (2016).
21. C. Mendelsohn, E. Batourina, S. Fung, T. Gilbert, J. Dodd, Stromal cells mediate retinoid-dependent functions essential for renal development. *Development* **126**, 1139–1148 (1999).
22. E. Sierra-Mondragon *et al.*, All-trans retinoic acid attenuates fibrotic processes by downregulating TGF-beta1/Smad3 in early diabetic nephropathy. *Biomolecules* **9**, 525 (2019).

23. N. M. Fiaschi-Taesch *et al.*, Prevention of acute ischemic renal failure by targeted delivery of growth factors to the proximal tubule in transgenic mice: The efficacy of parathyroid hormone-related protein and hepatocyte growth factor. *J. Am. Soc. Nephrol.* **15**, 112–125 (2004).
24. E. Jacquemin *et al.*, Pattern of expression of gamma-glutamyl transpeptidase in rat liver and kidney during development: Study by immunochemistry and in situ hybridization. *J. Pediatr. Gastroenterol. Nutr.* **11**, 89–95 (1990).
25. B. Chapellier *et al.*, A conditional floxed (loxP-flanked) allele for the retinoic acid receptor alpha (RARalpha) gene. *Genesis* **32**, 87–90 (2002).
26. S. K. Mallipattu, J. C. He, The beneficial role of retinoids in glomerular disease. *Front. Med. (Lausanne)* **2**, 16 (2015).
27. Q. Xu *et al.*, Retinoids in nephrology: Promises and pitfalls. *Kidney Int.* **66**, 2119–2131 (2004).
28. B. D. Humphreys *et al.*, Intrinsic epithelial cells repair the kidney after injury. *Cell Stem Cell* **2**, 284–291 (2008).
29. R. Kramann, T. Kusaba, B. D. Humphreys, Who regenerates the kidney tubule? *Nephrol. Dial. Transplant.* **30**, 903–910 (2015).
30. B. A. Naved *et al.*, Kidney repair and regeneration: Perspectives of the NIDDK (Re)Building a kidney consortium. *Kidney Int.* **101**, 845–853 (2022).
31. J. L. Zhuo, X. C. Li, Proximal nephron. *Compr. Physiol.* **3**, 1079–1123 (2013).
32. K. Kannan, S. K. Jain, Oxidative stress and apoptosis. *Pathophysiology* **7**, 153–163 (2000).
33. S. Dalleau, M. Baradat, F. Guéraud, L. Huc, Cell death and diseases related to oxidative stress:4-hydroxynonenal (HNE) in the balance. *Cell Death Differ.* **20**, 1615–1630 (2013).
34. T. Kimura *et al.*, Autophagy protects the proximal tubule from degeneration and acute ischemic injury. *J. Am. Soc. Nephrol.* **22**, 902–913 (2011).
35. G. P. Kaushal, S. V. Shah, Autophagy in acute kidney injury. *Kidney Int.* **89**, 779–791 (2016).
36. D. Bloemberg, J. Quadrilatero, Autophagy, apoptosis, and mitochondria: Molecular integration and physiological relevance in skeletal muscle. *Am. J. Physiol. Cell Physiol.* **317**, C111–C130 (2019).
37. A. Sureshbabu *et al.*, RIPK3 promotes sepsis-induced acute kidney injury via mitochondrial dysfunction. *JCI Insight* **3**, e98411 (2018).
38. V. J. Xavier, J. C. Martinou, RNA granules in the mitochondria and their organization under mitochondrial stresses. *Int. J. Mol. Sci.* **22**, 9502 (2021).
39. F. Joubert, N. Puff, Mitochondrial cristae architecture and functions: Lessons from minimal model systems. *Membranes (Basel)* **11**, 465 (2021).
40. C. Guo, L. Sun, X. Chen, D. Zhang, Oxidative stress, mitochondrial damage and neurodegenerative diseases. *Neural. Regen. Res.* **8**, 2003–2014 (2013).
41. J. M. Weinberg, M. A. Venkatachalam, N. F. Roeser, I. Nissim, Mitochondrial dysfunction during hypoxia/reoxygenation and its correction by anaerobic metabolism of citric acid cycle intermediates. *Proc. Natl. Acad. Sci. U.S.A.* **97**, 2826–2831 (2000).
42. S. Guerrero-Castillo *et al.*, The assembly pathway of mitochondrial respiratory chain complex I. *Cell Metab.* **25**, 128–139 (2017).
43. M. Mimaki, X. Wang, M. McKenzie, D. R. Thorburn, M. T. Ryan, Understanding mitochondrial complex I assembly in health and disease. *Biochim. Biophys. Acta* **1817**, 851–862 (2012).
44. M. J. Ryan *et al.*, HK-2: An immortalized proximal tubule epithelial cell line from normal adult human kidney. *Kidney Int.* **45**, 48–57 (1994).
45. P. Marchetti, Q. Fovez, N. Germain, R. Khamari, J. Kluza, Mitochondrial spare respiratory capacity: Mechanisms, regulation, and significance in non-transformed and cancer cells. *FASEB J.* **34**, 13106–13124 (2020).
46. V. S. Sabbisetti *et al.*, Blood kidney injury molecule-1 is a biomarker of acute and chronic kidney injury and predicts progression to ESRD in type I diabetes. *J. Am. Soc. Nephrol.* **25**, 2177–2186 (2014).
47. R. L. Chevalier, The proximal tubule is the primary target of injury and progression of kidney disease: Role of the glomerulotubular junction. *Am. J. Physiol. Renal Physiol.* **311**, F145–161 (2016).
48. I. Grgic *et al.*, Targeted proximal tubule injury triggers interstitial fibrosis and glomerulosclerosis. *Kidney Int.* **82**, 172–183 (2012).
49. A. B. Fogo, M. A. Lusco, B. Najafian, C. E. Alpers, AJKD atlas of renal pathology: Toxic acute tubular injury. *Am. J. Kidney Dis.* **67**, e31–e32 (2016).
50. M. Stevens, S. Oltean, Assessment of kidney function in mouse models of glomerular disease. *J. Vis. Exp.* **136**, 57764 (2018), 10.3791/57764.
51. W. C. Prozialeck, P. C. Lamar, D. M. Appelt, Differential expression of E-cadherin, N-cadherin and beta-catenin in proximal and distal segments of the rat nephron. *BMC Physiol.* **4**, 10 (2004).
52. L. Chen *et al.*, Central role of dysregulation of TGF-beta/Smad in CKD progression and potential targets of its treatment. *Biomed. Pharmacother.* **101**, 670–681 (2018).
53. H. Y. Lan, Smads as therapeutic targets for chronic kidney disease. *Kidney Res. Clin. Pract.* **31**, 4–11 (2012).
54. S. I. Kim, M. E. Choi, TGF-β-activated kinase-1: New insights into the mechanism of TGF-β signaling and kidney disease. *Kidney Res. Clin. Pract.* **31**, 94–105 (2012).
55. A. Sureshbabu, S. A. Muhsin, M. E. Choi, TGF-β signaling in the kidney: Profibrotic and protective effects. *Am. J. Physiol. Renal Physiol.* **310**, F596-f606 (2016).
56. J. L. Napoli, Retinoic acid: Sexually dimorphic, anti-insulin and concentration-dependent effects on energy. *Nutrients* **14**, 1553 (2022).
57. L. S. Gewin, Renal fibrosis: Primacy of the proximal tubule. *Matrix Biol.* **68–69**, 248–262 (2018).
58. W. Zhao, X. Wang, K. H. Sun, L. Zhou, α-smooth muscle actin is not a marker of fibrogenic cell activity in skeletal muscle fibrosis. *PLoS One* **13**, e0191031 (2018).
59. J. M. Starkey *et al.*, Altered retinoic acid metabolism in diabetic mouse kidney identified by O isotopic labeling and 2D mass spectrometry. *PLoS One* **5**, e11095 (2010).
60. M. Ostermann, M. Joannidis, Acute kidney injury 2016: Diagnosis and diagnostic workup. *Crit. Care* **20**, 299 (2016).
61. D. M. Widiatmaja *et al.*, The effect of long-term ketogenic diet on serum adiponectin and insulin-like growth factor-1 levels in mice. *J. Basic Clin. Physiol. Pharmacol.* **33**, 611–618 (2021), 10.1515/jbcpp-2021-0287.
62. S. Lopez-Giacoman, M. Madero, Biomarkers in chronic kidney disease, from kidney function to kidney damage. *World J. Nephrol.* **4**, 57–73 (2015).
63. C. P. Argyropoulos *et al.*, Rediscovering beta-2 microglobulin as a biomarker across the spectrum of kidney diseases. *Front. Med. (Lausanne)* **4**, 73 (2017).
64. P. V. Bhat, D. C. Manolescu, Role of vitamin A in determining nephron mass and possible relationship to hypertension. *J. Nutr.* **138**, 1407–1410 (2008).
65. P. Bhargava, R. G. Schnellmann, Mitochondrial energetics in the kidney. *Nat. Rev. Nephrol.* **13**, 629–646 (2017).
66. J. Finsterer, F. A. Scorza, Renal manifestations of primary mitochondrial disorders. *Biomed. Rep.* **6**, 487–494 (2017).
67. D. Bhatia, A. Capili, M. E. Choi, Mitochondrial dysfunction in kidney injury, inflammation, and disease: Potential therapeutic approaches. *Kidney Res. Clin. Pract.* **39**, 244–258 (2020).
68. B. Chidipi *et al.*, All-trans retinoic acid increases DRP1 levels and promotes mitochondrial fission. *Cells* **10**, 1202 (2021).
69. M. Tran *et al.*, PGC-1alpha promotes recovery after acute kidney injury during systemic inflammation in mice. *J. Clin. Invest.* **121**, 4003–4014 (2011).
70. H. Hartmannová *et al.*, Acadian variant of Fanconi syndrome is caused by mitochondrial respiratory chain complex I deficiency due to a non-coding mutation in complex I assembly factor NDUFAF6. *Hum. Mol. Genet.* **25**, 4062–4079 (2016).
71. B. Thompson *et al.*, Genetics and functions of the retinoic acid pathway, with special emphasis on the eye. *Hum. Genomics* **13**, 61 (2019).
72. A. Chen, Y. Liu, Y. Lu, K. Lee, J. C. He, Disparate roles of retinoid acid signaling molecules in kidney disease. *Am. J. Physiol. Renal Physiol.* **320**, F683–F692 (2021).
73. Y. Kirita, H. Wu, K. Uchimura, P. C. Wilson, B. D. Humphreys, Cell profiling of mouse acute kidney injury reveals conserved cellular responses to injury. *Proc. Natl. Acad. Sci. U.S.A.* **117**, 15874–15883 (2020).
74. D. Bhatia *et al.*, Mitophagy-dependent macrophage reprogramming protects against kidney fibrosis. *JCI Insight* **4**, e132826 (2019).
75. A. S. Chang, C. K. Hathaway, O. Smithies, M. Kakoki, Transforming growth factor-β1 and diabetic nephropathy. *Am. J. Physiol. Renal Physiol.* **310**, F689–F696 (2016).
76. Y. Wang *et al.*, Evaluation of the safety and tolerability of tamoxifen for ischemia-incited renal injury in mice. *Am. J. Transl. Res.* **10**, 2184–2194 (2018).
77. F. J. Rosales, S. J. Ritter, R. Zolfaghari, J. E. Smith, A. C. Ross, Effects of acute inflammation on plasma retinol, retinol-binding protein, and its mRNA in the liver and kidneys of vitamin A-sufficient rats. *J. Lipid Res.* **37**, 962–971 (1996).
78. M. J. Lewandowski *et al.*, Chronic kidney disease is more prevalent among women but more men than women are under nephrological care: Analysis from six outpatient clinics in Austria 2019. *Wien. Klin. Wochenschr.* **135**, 89–96 (2023).
79. M. Schaier, T. Jocks, H. J. Grone, E. Ritz, J. Wagner, Retinoid agonist isotretinoin ameliorates obstructive renal injury. *J. Urol.* **170**, 1398–1402 (2003).
80. K. Kishimoto *et al.*, Therapeutic effect of retinoic acid on unilateral ureteral obstruction model. *Nephron Exp. Nephrol.* **118**, e69–e78 (2011).
81. S. E. Trasino, X.-H. Tang, M. M. Shevchuk, M. E. Choi, L. J. Gudas, Amelioration of diabetic nephropathy using a retinoic acid receptor β_2 agonist. *J. Pharmacol. Exp. Ther.* **367**, 82–94 (2018).
82. K. K. Ratnam *et al.*, Role of the retinoic acid receptor-alpha in HIV-associated nephropathy. *Kidney Int.* **79**, 624–634 (2011).
83. Y. Zhong *et al.*, Novel retinoic acid receptor alpha agonists for treatment of kidney disease. *PLoS One* **6**, e27945 (2011).
84. A. R. Sepulveda, B. Z. Carter, G. M. Habib, R. M. Lebovitz, M. W. Lieberman, The mouse gamma-glutamyl transpeptidase gene is transcribed from at least five separate promoters. *J. Biol. Chem.* **269**, 10699–10705 (1994).
85. X. H. Tang *et al.*, A retinoic acid receptor β2 agonist attenuates transcriptome and metabolome changes underlying nonalcohol-associated fatty liver disease. *J. Biol. Chem.* **297**, 101331 (2021).
86. K. M. Dikun *et al.*, Retinoid levels measurement in kidney and serum. National Metabolomics Data Repository (NMDR). https://doi.org/10.21228/M8WQ6G. Deposited 14 January 2024.